Soft Matter

PAPER

View Article Online
View Journal | View Issue

Cite this: *Soft Matter*, 2024, **20**, 7199

Theory and quantitative assessment of pH-responsive polyzwitterion–polyelectrolyte complexation†

Samuel C. Hoover,[a] Khatcher O. Margossian ‡[bc] and Murugappan Muthukumar *[b]

Received 14th May 2024,
Accepted 20th August 2024

DOI: 10.1039/d4sm00575a

rsc.li/soft-matter-journal

We introduce a theoretical framework to describe the pH-sensitive phase behavior of polyzwitterion–polyelectrolyte complex coacervates that reasonably captures the phenomenon from recent experimental observations. The polyzwitterion is described by a combinatorial sequence of the four states in which each zwitterionic monomer can occupy: dipolar, quasi-cationic, quasi-anionic, and fully neutralized. We explore the effects of various modifiable chemical and physical properties of the polymers—such as, pK_a of the pH-active charged group on the zwitterion, equilibrium constant of salt condensation on the permanently charged group on the zwitterion, degrees of polymerization, hydrophobicity (*via* the Flory–Huggins interaction parameter), and dipole lengths—on the window of complexation across many stoichiometric mixing ratios of polyzwitterion and polyelectrolyte. The properties that determine the net charge of the polyzwitterion have the strongest effect on the pH range in which polyzwitterion–polyelectrolyte complexation occurs. We finish with general guidance for those interested in molecular design of polyzwitterion–polyelectrolyte complex coacervates and opportunities for future investigation.

1 Introduction

Nearly a century has elapsed since complex coacervation was first described and studied in the Netherlands.[1] Since then, a wealth of knowledge has been borne out through rigorous experimental, theoretical, and simulation studies.[2–8] This phenomenon is attributed to the liquid–liquid phase separation that occurs between oppositely charged macromolecules. Briefly, favorable electrostatic interactions between the oppositely charged chains are augmented by the entropically favorable release of counterions to produce the characteristic polymer-rich and polymer-poor phases seen in these self-assembling systems.[9,10] Coacervates, as well as coacervate-based systems, represent an intriguing class of materials which can be used in various industrial settings as carriers of biomedical cargoes,[11–14] adhesives,[15–17] electronic inks,[18,19] food additives,[20,21] and so on. Moreover, in more fundamental contexts, these self-assembling droplets offer unique insights into the solution-state behavior of charged polymers, and their physics may even answer longstanding questions about human disease (within the context of protein aggregates, disordered proteins, and biomolecular condensates)[22–29] and the origins of life in the pre-cellular Earth.[30–33]

The rich phase behavior of coacervates is a result of their delicate nature, many interacting components, and multiple scales in time, length, and energy in which coacervation occurs. Solution pH is one of the many parameters to which macromolecules participating in coacervation are sensitive, as it determines the charge density of the polyelectrolyte.[34–39] Under typical circumstances, coacervate droplets are stable near a neutral pH. For polyanions and polycations to interact, both participants should achieve their maximally charged states, which is normally at a pH value that is between the pK_a values of the two types of chains. When one chain is under-charged (when the ambient pH is pushed too high or too low), it can no longer participate in the electrostatic interactions that lead to complexation – the coacervate droplets dissolve. However, leveraging and extending these ideas, recent work has shown that it is possible to induce coacervation at remarkably low pH values (<4) by using a polyzwitterion *in lieu* of a polycation to form the phase-separated polymer droplets.[40] An illustration of

[a] *Department of Chemical Engineering, University of Massachusetts Amherst, Amherst, MA 01003, USA*
[b] *Department of Polymer Science and Engineering, University of Massachusetts Amherst, Amherst, MA 01003, USA. E-mail: muthu@polysci.umass.edu*
[c] *Rush University Medical Center and John H. Stroger Hospital of Cook County, both in Chicago, IL 60612, USA*

† Electronic supplementary information (ESI) available: Derivations for probabilties of zwitterion states, degrees of ionization, and phase behavior constraint equations for free energy minimization. See DOI: https://doi.org/10.1039/d4sm00575a

‡ Present address: Rush University Medical Center and John H. Stroger Hospital of Cook County, both in Chicago, IL 60612, USA.

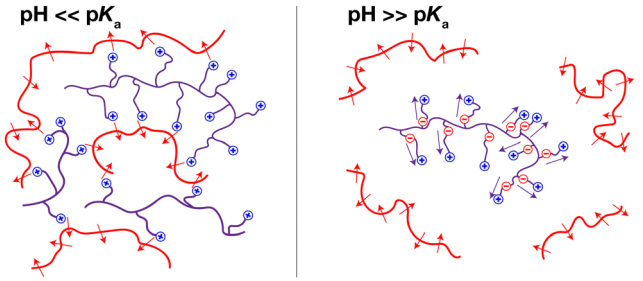

Fig. 1 Illustration of our model system. Our system consists of polyzwitterions (purple curves), protonated polyanions (*i.e.*, polydipoles; red curves), positive and negative monovalent salt ions (not shown), and solvent (not shown). The charged groups of the polyzwitterion are depicted as blue positive symbols and red negative symbols tethered to the backbone. The negative moiety is the pH-active group on each zwitterionic monomer while the positive moiety is a permanent charge, subjected only to small salt ion condensation reactions. Left: At a pH sufficiently lower than the pK_a of the negative moiety on the zwitterion, the negative charges of the polyzwitterion are neutralized and complexation between polyzwitterions and dipolar polyanions occurs, forming polyzwitterionic complexes (pZCs). Right: Once the pH is raised to be sufficiently higher than the pK_a of the negative moiety on the zwitterion, the negative charges on the polyzwitterion are ionized. Thus, the polyzwitterion monomers adopt a dipolar state and, concurrently, the pZC dissociates. It is important to note that the orientation of the charged groups along the side chain is not taken into consideration in our theory. Adapted from K. O. Margossian *et al.*, *Nat. Commun.*, 2022, **13**, 2250. Licensed under CC BY 4.0.

that system can be seen in Fig. 1. Critically, this polyzwitterionic complex ("pZC") system displays pH sensitivity that lends its usefulness for future gastrointestinal drug delivery applications.

Briefly, past work[40] illustrated the emergence of complexation between pMPC, which is a polyzwitterion with phosphorylcholine monomers, and poly(acrylic acid) (pAA) at low pH. Interestingly, at pH values that exceed a threshold value (in this case, around 4), these complexes disassemble in a controllable fashion. Aside from the drug delivery technologies that may harness such phase behavior, counter-intuitive physics emerged from this phenomenon. At the pH ranges in which complexation was observed, the polyzwitterion's phosphoryl group was sufficiently protonated so as to render many of the zwitterionic monomers as cationic, with the quaternary amine serving as the lone charged entity on those monomers. Conversely, at this low pH, the pAA monomers were also protonated, which effectively neutralized nearly all of their negative charges. That said, even when protonated, pAA contains an appreciable dipole moment, and this dipole moment can evidently undergo coacervation with the charged amine on pMPC to form pZCs. Despite the comparative weakness of such charge–dipole interactions (as compared to more conventional charge–charge interactions seen coacervates), these complexes are thermodynamically favorable at low pH values (in this system, at pH < 4), and exhibit many of the same properties seen in coacervates that exist at much higher pH ranges. That said, to expand upon prior work in characterizing the underlying physics of pZC systems, we turn to a theoretical and computational approach that can rapidly determine (1) if charges and dipoles can indeed phase-separate with one another in the first place, and (2) what controls the nuances of such phase-separating systems, at least in terms of chemically modifiable properties of the constituent chains, such as degree of polymerization, backbone hydrophobicity, dipole moment, *etc.* With this study, we hope to bolster the theoretical backbone that explains some of the salient features of pZC formation, and provide chemists and engineers with actionable handles by which they can design controllable pZC systems that are tailored for their specific goals.[41] More generally, although the bulk of this paper deals within the relatively narrow context of pZCs, we recognize that nearly-identical physics can explain the phase separation of other polyampholytes, such as the proteins that interact with one another to give rise to neurodegenerative disorders like Alzheimer's disease, Lewy Body dementia, and Parkinson's disease.

The applicability of pZCs need not be limited to the delivery of pharmaceuticals *via* the oral route. Pathological triggers allow researchers to exploit the specific chemical or physical markers of a particular disease for the purpose of developing useful drug delivery platforms. For example, a hallmark for cancerous tissue is its lower extracellular pH (<6.5) than that of healthy tissue (7.3–7.5).[42,43] While much work has focused on leveraging pH gradients with respect to drug delivery, non-pharmaceutical applications for pH-triggered release also exist. Polyelectrolytes can be used to coat microscale bioreactors to regulate enzymatic reactions *via* pH.[44] The pH shift during the curing process of ammonia-containing coatings can be used to induce additional properties.[45] Other coating applications which mitigate the effects of acidic corrosion or improve battery electrode performance[46] can also be easily envisioned. Additionally, cosmetic and hygiene products can also exploit the pH difference between healthy skin (which is weakly acidic) and sweat (neutral pH) for the release of fragrances upon perspiration.[47,48]

In this study, we present a theoretical model to study the phase behavior of pZCs as they respond to various chemical and physical properties. We assess the manner in which chemical context can influence the propensity of these systems to phase separate through dipolar interactions. The main thrust of our model is the treatment of the polyzwitterion as a combinatorial sequence of four possible states: (1) zwitterionic, (2) quasi-cationic, (3) quasi-anionic, and (4) fully neutralized. These states are depicted in Fig. 2.

To determine if our model is capable of capturing the pH-sensitive behavior of pZCs, we construct numerous phase diagrams in which we systematically investigate the effect of individual parameters that are known to promote or suppress complexation in charged macromolecules. We find that our model generally agrees with the experimentally-observed pH-dependent properties in previous work. Furthermore, we also make several experimentally accessible predictions about the phase separation of polyzwitterion–polyelectrolyte systems with a wide variety of unique properties.

The manuscript is organized as follows. In Section 2, we first introduce our model system and non-electrostatic contributions to our free energy expression. Next, in Section 2.1, we describe our treatment of the polyzwitterion and the

electrostatic contributions to the free energy. In Section 3 we identify the modifiable and chemically relevant parameters and then study and discuss their effects on complexation between polyzwitterions and polyelectrolytes. Finally, in Section 4, we conclude with our findings and discuss future work.

2 Model and theory

We consider a system of polyzwitterions, dipolar polyanions, ions from the acidic environment, and solvent. To simplify our accounting, we assume that the pK_a of the polyanion is sufficiently high relative to the highest pH considered. In doing so, we treat the polyanion (and its counterions) as a chain of dipoles, as depicted in Fig. 1. All system species (monomers, ions, and solvent molecules) are assumed to have an identical size, length ℓ, and the system is considered to be incompressible. Although prior work[49–54] has noted rich variability in the dielectric properties of the local environment around polymer chains, for the sake of computational tractability, the dielectric constant of our solvent, ε, is assumed to be globally constant.

The free energy density f of our system, assuming a homogeneous solution, follows closely to that from Adhikari, Leaf, and Muthukumar,[55]

$$f = f_{S,p} + f_{S,i} + f_{S,0} + f_{el} + f_{ex} + f_{fl,i}. \quad (1)$$

The first three terms on the right-hand side of eqn (1) describe the entropy of mixing, the fourth and fifth describe the enthalpic contributions, and the final describes the charge fluctuation. The entropy arising from the conformations of the polymer species, $f_{S,p}$, is

$$f_{S,p} = \frac{\phi_1}{N_1}\ln\phi_1 + \frac{\phi_2}{N_2}\ln\phi_2, \quad (2)$$

where the subscripts "1" and "2" refer to the polyzwitterion and polydipole, respectively, and ϕ_i and N_i are the volume fraction and number of Kuhn segments per chain of species i, respectively. Entropy from mobile ions in solution, $f_{S,i}$, is

$$f_{S,i} = \phi_{+,soln}\ln\phi_{+,soln} + \phi_{-,soln}\ln\phi_{-,soln}, \quad (3)$$

where $\phi_{+,soln}$ and $\phi_{-,soln}$ are the volume fractions of the positive and negative ions in solution, respectively. The final entropic contribution, that from the solvent, $f_{S,0}$ is

$$f_{S,0} = \phi_0\ln\phi_0, \quad (4)$$

where ϕ_0 is the volume fraction of the solvent.

The theoretical framework that we use is applicable only to systems of polyelectrolytes. The introduction of polyzwitterion into our system *in lieu* of polycation requires that the expression for the electrostatic contribution be revised due to the polyzwitterion containing one negative and one positive charge on each repeat unit as opposed to the single positive charge on each repeat unit of the polycation. The zwitterionic monomer consists of one pH-active charge group – in our case, the negative moiety – and one permanent charge that is subjected to salt ion condensation reactions[49,50,56–64] – the positive moiety – as opposed to acid–base reactions.[51,65] It must be noted that there is no fundamental difference between the association of a proton to an anion and the binding of a counterion to a charged group, since both arise from the same fundamental electrostatic interaction. We allow each zwitterionic monomer to occupy one of four states as illustrated in Fig. 2. In doing so, we treat each polyzwitterion chain as a sequence of states A–D where the fraction of each chain that is in state i is dependent upon system conditions like pH, pK_a of the negative moiety on the zwitterion (hereafter, simply referred to as pK_a), Bjerrum length (defined below), *etc.* It must be noted that we assume there are no sequence-dependent interactions within or without the polyzwitterion. Only the fraction of the polyzwitterion belonging to each state contributes to the free energy. Therefore, two polyzwitterions (both $N = 5$) with sequences A–B–B–C–A and B–A–B–A–C are identical since we consider the sequence (*i.e.*, polyzwitterion) to be a combination rather than a permutation. A full description of the electrostatics will be provided in Section 2.1.

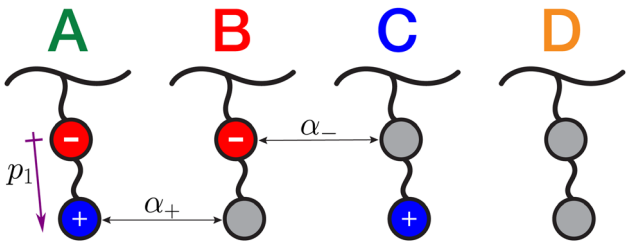

Fig. 2 The four states a zwitterionic monomer can occupy. The degree of ionization of the red negative moiety is defined by α_- while that of the blue positive moiety is α_+. Grey symbols represent a neutralized charged group. The charge of state i, q_i, is determined by the presence and/or absence of the charged moieties. In state A, both charged moieties are ionized, forming a dipole moment with a dipole length p_1; the zwitterion is in its "natural" state, $q_A = 0$. In state B, only the positive moiety is neutralized; the zwitterion acts as a quasi-anion, $q_B = -1$. In state C, only the negative moiety is neutralized; the zwitterion acts as a quasi-cation, $q_C = +1$. In state D, both charged group are neutralized; the zwitterion is fully neutralized, $q_D = 0$.

Continuing with the rest of our free energy density expression, the excluded volume contribution, f_{ex}, accounts for chemical mismatch between the two polymer species and the hydrophobicity of each polymer (our solvent is water),

$$f_{ex} = \chi_{12}\phi_1\phi_2 + \chi_{10}\phi_1\phi_0 + \chi_{20}\phi_2\phi_0, \quad (5)$$

where χ_{ij} is the Flory–Huggins interaction parameter between species i and j. The fluctuation contribution from the free ions around the polymers, $f_{fl,i}$, is defined as

$$f_{fl,i} = -\frac{1}{4\pi}\left[\ln(1+\kappa\ell) - \kappa\ell + \frac{1}{2}(\kappa\ell)^2\right], \quad (6)$$

where κ is the inverse Debye length and ℓ is the Kuhn length. The inverse Debye length for each phase is given by

$$\kappa^2 = \frac{4\pi\ell_B}{\ell^3}(\phi_{+,soln} + \phi_{-,soln}), \quad (7)$$

where $\ell_B = e^2/4\pi\varepsilon_o\varepsilon k_B T$ is the Bjerrum length, e is the elementary charge, ε_o is the vacuum permittivity, k_B is the Boltzmann constant, and T is the absolute temperature. To determine

the dielectric constant of water, we use the definition from Malmberg and Maryott.[66] At 298 K, the temperature we considered, $\varepsilon = 78.3$.

2.1 Electrostatic interactions

The electrostatic contributions are limited to the two-body interactions of charge–charge, charge–dipole, and dipole–dipole interactions, denoted by the subscripts ''cc'', ''cd'', and ''dd'', respectively,

$$f_{\mathrm{el}} = f_{\mathrm{el,cc}} + f_{\mathrm{el,cd}} + f_{\mathrm{el,dd}}. \tag{8}$$

In the derivation for the dipolar interactions, we take the high temperature expansion and assume freely rotating dipoles such that dipole orientation has no effect on the electrostatic contributions. Therefore, the orientation of the charged groups – whether the negatively charged group is proximal to the backbone and the positively charged group distal to it or *vice versa* – is not taken into consideration in our theory. We also ignore any steric hindrance effects that may dissuade interactions with the charged group proximal to the backbone.

The probability of each state, denoted by $\mathbb{R}_i$, where i = A, B, C, D, is calculated using the Boltzmann weight of each state. Doing so, we arrive at the following ratio,

$$\frac{\mathbb{R}_{\mathrm{A}}\mathbb{R}_{\mathrm{D}}}{\mathbb{R}_{\mathrm{B}}\mathbb{R}_{\mathrm{C}}} = e^{\ell_{\mathrm{B}}/p_1}, \tag{9}$$

where p_1 is the dipole length of the zwitterionic monomer. Defining three additional constraint equations,

$$\begin{aligned} \mathbb{R}_{\mathrm{A}} + \mathbb{R}_{\mathrm{B}} + \mathbb{R}_{\mathrm{C}} + \mathbb{R}_{\mathrm{D}} &= 1, \\ \mathbb{R}_{\mathrm{A}} + \mathbb{R}_{\mathrm{C}} &= \alpha_+, \\ \mathbb{R}_{\mathrm{A}} + \mathbb{R}_{\mathrm{B}} &= |\alpha_-|, \end{aligned} \tag{10}$$

we can solve for the probability of each zwitterionic state. Details about the derivation can be found in ESI,† Section S1.

Both degrees of ionization will be pH-dependent as the pH directly dictates the number of mobile ions, both positive and negative, in the system available to interact with the charged groups on the zwitterion. The pK_{a} value will parameterize α_- while the equilibrium constant of salt condensation, K_{salt}, onto the positive moiety will parameterize α_+. Using the Henderson–Hasselbalch equation, the definition for α_-, the degree of ionization of the negative moiety on the zwitterion, can be determined,

$$\alpha_- = -\frac{1}{1 + 10^{\mathrm{p}K_{\mathrm{a}} - \mathrm{pH}}}. \tag{11}$$

The definition for α_+, the degree of ionization of the positive moiety on the zwitterion, can be reached by considering a general chemical equation for the condensation of a small negative salt ion onto the positively charged group of the zwitterion,

$$\alpha_+ = \frac{1}{1 + K_{\mathrm{salt}} \times 10^{-\mathrm{pH}}}. \tag{12}$$

The subsequent details for the derivations of both degrees of ionization can be found in ESI,† Section S2.

Combining our definitions for $\mathbb{R}_i$, α_+, and α_-, we can finally determine the probability distributions of each zwitterion state as a function of pH. We chose a pK_{a} of 2.3 and a K_{salt} of 25 as those values correspond to the chemical details of the motivating experimental work.[40] The number for K_{salt} comes from corresponding literature values for the simpler system, tetramethylammonium chloride,[67] since an explicit value for MPC (2-methacryloyloxyethyl phosphorylcholine) chloride has not been yet experimentally determined. The probability distributions, degrees of ionization, and the net charge of the polyzwitterion – all as a function of pH – can be seen in Fig. 3. The net charge of the polyzwitterion, Q_1, is calculated using a probability weighted sum of the charge of each zwitterion state, $Q_1 = \sum_i q_i \mathbb{R}_i$ where q_i is the charge of state i.

We want to understand the effects of pertinent system conditions on the effective charge of the polyzwitterion. Relevant system conditions include temperature (which manifests in the Bjerrum length), p_1, K_{salt}, and pK_{a}, and, of course, pH. To do so, we calculated the probability distributions of each zwitterion state while varying each parameter individually. Referring to Fig. 4, we find that both parameters on the right-hand side of eqn (9), p_1 and ℓ_{B}, have minimal effects towards the probability distributions when varied over physically relevant values.

The parameters that directly effect α_+ and α_- (K_{salt} and pK_{a}, respectively) have the greatest influence. The pK_{a} value dramatically influences the effective charge of the polyzwitterion. Not only does it greatly increase the probability of the polyzwitterion adopting a quasi-polycationic state, it also broadens the pH range in which it primarily adopts that state. From Fig. 5, it is evident only K_{salt} and pK_{a} have any effect on the net charge of the polyzwitterion. As K_{salt} increases, the polyzwitterion maximal charge decreases while the pH at which the polyzwitterion is maximally charged increases. This is due to α_+ decreasing as K_{salt} is increased, thus making states B and D more favorable, and requiring a higher pH for the zwitterions to shed their counterions. As pK_{a} increases, the polyzwitterion maximal charge and the pH at which the polyzwitterion is maximally charged both increase. State C becomes significantly more favorable with increasing pK_{a} since the negative moiety will hold onto its counterion longer as pH is increased. As Q_1 asymptotically approaches net-neutral (*i.e.*, the polyzwitterion monomers adopts the dipolar state), we expect to see the cessation of pZC formation following the arguments from the authors of the experimental work.

Now that we have values for each of the $\mathbb{R}_i$ in our system, it is possible to fully describe the electrostatic contribution to our free energy density expression. The reason for this approach is to calculate the volume fraction of the polyzwitterion that is available for certain interactions, whether it be charge–charge, charge–dipole, or dipole–dipole. Obviously, a zwitterion that is in state C, a quasi-cation, cannot participate in dipole–dipole interactions, but it can participate in charge–charge or charge–dipole. Thus, $\mathbb{R}_{\mathrm{B}}$ shows up in those respective electrostatic expressions. To get the electrostatic contributions from each type of interaction, we consider the relevant prefactors, charge

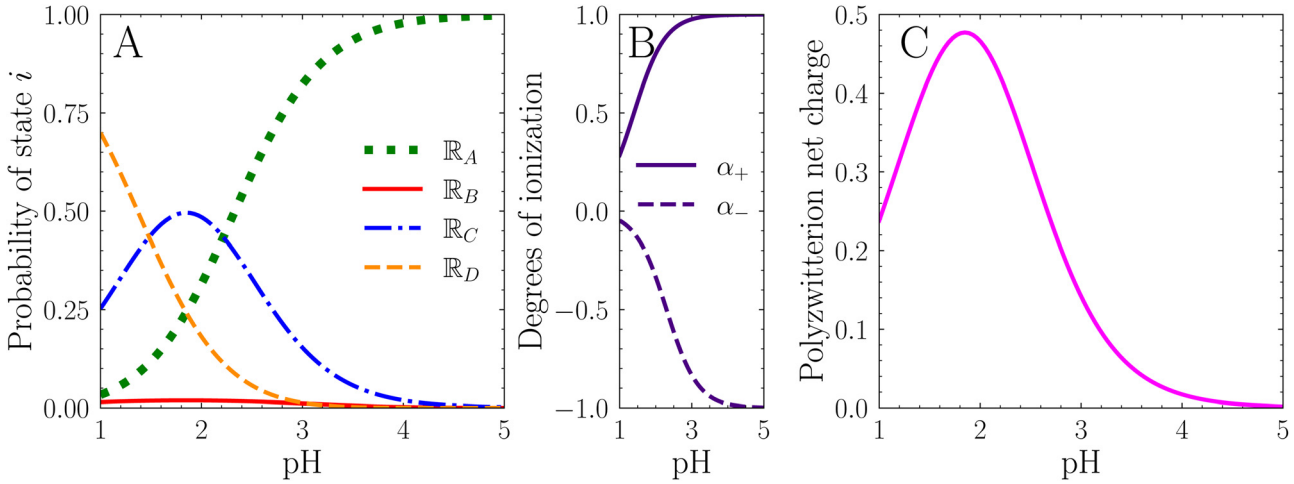

Fig. 3 Details of the effective charge of the polyzwitterion as a function of pH. Refer back to Fig. 2 for an illustration of each zwitterion case. (A) The probability distribution for each state. At the lower pH range, pH < 2, the negative moiety is considerably neutralized, indicated by the predominance of states C and D. As pH approaches the pK_a value, the polyzwitterion monomers increasingly adopts the dipolar state until around pH 4, where the polyzwitterion is essentially a chain of dipoles. (B) The degrees of ionization as a function of pH. Here, we use K_{salt} = 25 and pK_a = 2.3. We lump the charge of the charged group along with its degree of ionization. Hence, $\alpha_+ \in [0,1]$ while $\alpha_- \in [-1,0]$. (C) The net charge of the polyzwitterion, Q_1, can be determined using a probability weighted sum of the charge of each zwitterion state, $Q_1 = \sum_i q_i \mathbb{R}_i$. The polyzwitterion reaches its maximally charged state around pH 1.8.

(if necessary), probability of each state, dipole lengths, and the relevant volume fractions:

$$f_{el,cc} = v_{cc}\left[\frac{1}{2}(q_B\mathbb{R}_B\phi_1)^2+\frac{1}{2}(q_C\mathbb{R}_C\phi_1)^2+\frac{1}{2}q_Bq_C\mathbb{R}_B\mathbb{R}_C{\phi_1}^2\right]$$

$$f_{el,cd} = v_{cd}\left[\frac{1}{2}\mathbb{R}_A\mathbb{R}_B{p_1}^2{\phi_1}^2+\mathbb{R}_E\mathbb{R}_B{p_2}^2\phi_1\phi_2 + \frac{1}{2}\mathbb{R}_A\mathbb{R}_C{p_1}^2{\phi_1}^2+\mathbb{R}_E\mathbb{R}_C{p_2}^2\phi_1\phi_2\right]$$

$$f_{el,dd} = v_{dd}\left[\frac{1}{2}\left(\mathbb{R}_A{p_1}^2\right)^2{\phi_1}^2+\frac{1}{2}\left(\mathbb{R}_E{p_2}^2\right)^2{\phi_2}^2+\mathbb{R}_A\mathbb{R}_E{p_1}^2{p_2}^2\phi_1\phi_2\right]. \quad (13)$$

In the above expressions, $\mathbb{R}_E$ is the probability of the polyanion being in its protonated (*i.e.*, dipolar) state. Since we assume the pK_a value of the charged groups of the polyanion to be sufficiently higher than the pH values considered in this study, $\mathbb{R}_E$ = 1. Additionally, p_2 is the dipole length of the polydipole and v_{cc}, v_{cd}, and v_{dd} are the pseudopotentials that parameterize the strength of charge–charge, charge–dipole, and dipole–dipole interactions, respectively.[53] Notably, the treatment of the polyanion as a chain of dipoles allows us to make several conclusions. With the exclusive focus on the weaker of the two charge-containing electrostatic interactions (charge–dipole rather than charge–charge), we can definitively state that if interactions between the two polymers do arise, the polydipolar system, though comparatively weaker, is indeed strong enough to sustain interactions with a charged entity, and that these interactions do not arise from residual anionic groups on the polyanion that could be driving the phase separation in the calculations herein. The definitions of the pseudopotentials are enumerated below:

$$v_{cc} = \frac{4\pi\ell_B}{\kappa^2\ell^3},$$

$$v_{cd} = -\frac{\pi}{3}\frac{{\ell_B}^2}{\ell^4}e^{-2\kappa\ell}(2+\kappa\ell), \quad (14)$$

$$v_{dd} = -\frac{\pi}{9}\frac{{\ell_B}^2}{\ell^6}e^{-2\kappa\ell}\left[4+8\kappa\ell+4(\kappa\ell)^2+(\kappa\ell)^3\right].$$

When phase separation occurs, there are 11 variables (a ϕ_1, ϕ_2, ϕ_+, ϕ_-, and ϕ_0 for each phase as well as x, the volume fraction of one of the two phases) and seven constraints (two incompressibility conditions, one electroneutrality condition, and four lever rules). Therefore, the free energy density of the system is minimized with respect to four independent variables. The constrained, multidimensional nonlinear minimization of the free energy density equation (eqn (1)) was performed using the Nelder–Mead method.[68] Details of the constraint equations are provided in ESI,† Section S3.

3 Results and discussion

Although typical phase diagrams are useful to conceptualize the behavior of polymeric system across various temperature and salt concentrations, in systems such as the ones being investigated, it behooves us to consider phase diagrams whose axes represent more chemically relevant variables. In the case of pZCs, because two polymers (namely, the polyzwitterion and the polyelectrolyte) are necessary for phase separation to occur, we consider the volume fractions of both polymers simultaneously by using the stoichiometric mixing ratio – defined as $\phi_1/(\phi_1+\phi_2)$ – between polyzwitterion and polydipole.

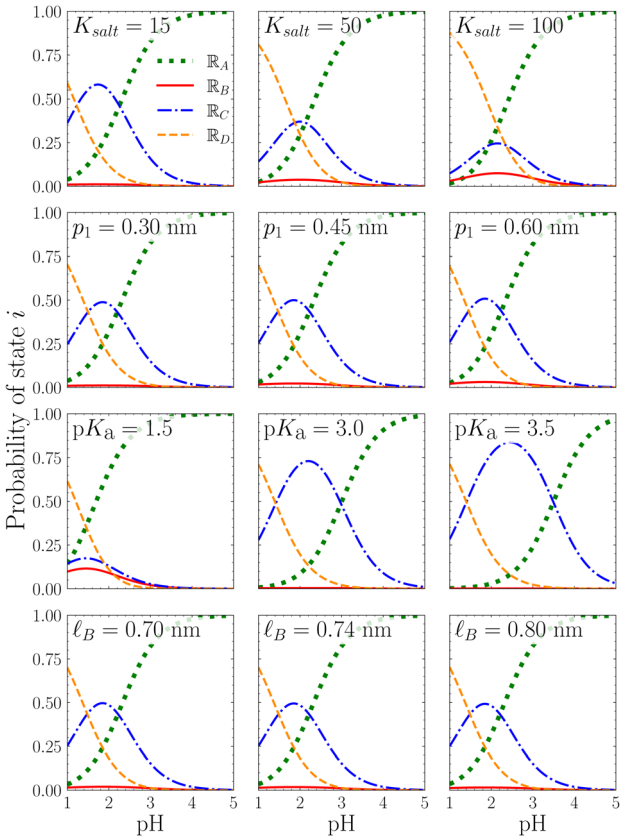

Fig. 4 Zwitterion state probability distributions with respect to key parameters. Moving downward row-wise, the effect of: K_{salt}, p_1, pK_a, and temperature. The parameters for each set of probability distributions are enumerated as follows, unless noted otherwise: T = 298 K, p_1 = 0.39 nm, K_{salt} = 25, and pK_a = 2.3. Temperature is related to ℓ_B and at 298 K, ℓ_B = 0.72 nm. The temperatures which correspond to ℓ_B = 0.70, 0.74, and 0.80 nm are 273, 323, and 373 K, respectively.

What is gained by constructing the phase diagrams in this manner is the fact that the influence of both polymers on phase behavior can be seen in one diagram. If only one polymer was treated at a time, it would be harder to draw definitive conclusions about the phase separation boundaries of the system as a whole, and would thus make the applicability of these phase diagrams to real chemical systems more indirect. That said, one piece of information that is lost is the ability to determine the polymer concentration of each phase from a single diagram. However, this information is not crucial for someone trying to simply formulate a particular pZC system from the starting configuration of polymer stoichiometry.

In order to learn what levers are at our disposal for pZC design, we have constructed multiple phase diagrams to understand the effect of chemically and experimentally relevant parameters on their phase behavior in Fig. 6–13. Namely, we are concerned with the chain lengths, their asymmetry, the hydrophobicity of both polymer species, the pK_a of the negative moiety on the zwitterion, K_{salt} of the positive moiety on the zwitterion, and the dipole lengths of the polymers. In all of our calculations, we take ℓ = 0.6 nm, χ_{12} = 0, and ignore chemical mismatch interactions involving ions.

3.1 Model captures pH-responsive polyzwitterion–polyelectrolyte complexation

Upon the minimization of the free energy density and construction of the phase diagram, we predict phase behavior that is in good qualitative agreement with the experimental observations. To establish the effect of the various parameters, we first need to establish a baseline. For the baseline case, we take $N_1 = N_2 = 100$, $\chi_{10} = \chi_{20} = 0.4$ (moderately hydrophobic polyzwitterion and polydipole), p_1 = 0.39 nm, p_2 = 0.0354 nm, pK_a = 2.3, and K_{salt} = 25. The values for dipole lengths, pK_a, and K_{salt} were chosen to match with the physical and chemical details of the experimental system. In most of our calculations, we typically consider the range pH 2 to pH 4, again to follow the experimental observations. Regardless of the pH, we assume the pK_a value of the charged group on the polyanion is sufficiently high such that the chain is negligibly ionized, and, thus, able to be treated as a chain of dipoles. In a few instances, we consider a slightly different pH values so as to fully capture the window of complexation. For example, to determine the effect of pK_a (Section 3.5), we consider the range pH 2 to pH 5 when we increase the pK_a value and pH 1 to pH 4 when we decrease the pK_a value. Each point represents a set of stoichiometric ratio value and pH value where complexation is found. Conversely, the

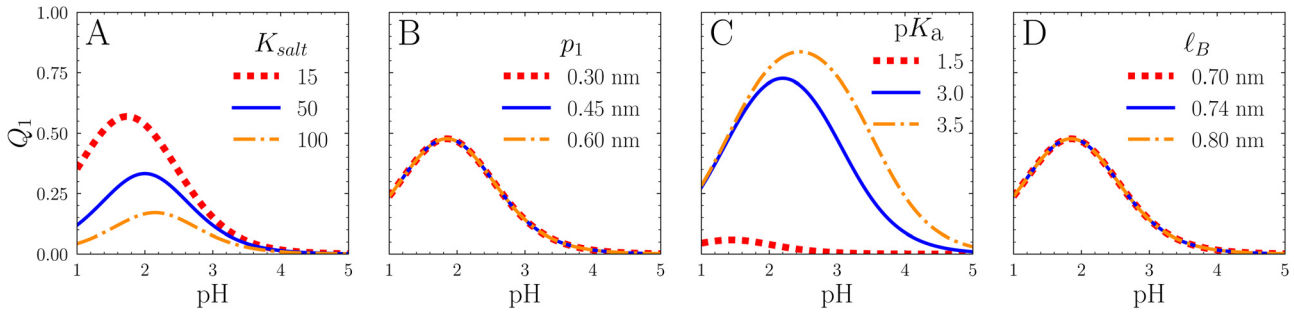

Fig. 5 Net charge of the polyzwitterion with respect to the key parameters. Similar to Fig. 4, the parameters for each Q_1 curve are enumerated as follows, unless noted otherwise: T = 298 K, p_1 = 0.39 nm, K_{salt} = 25, and pK_a = 2.3. Temperature is related to ℓ_B and at 298 K, ℓ_B = 0.72 nm. Effects of (A) K_{salt}, (B) dipole length of the zwitterionic monomer, (C) pK_a, and (D) temperature on Q_1. The temperatures which correspond to ℓ_B = 0.70, 0.74, and 0.80 nm are 273, 323, and 373 K, respectively.

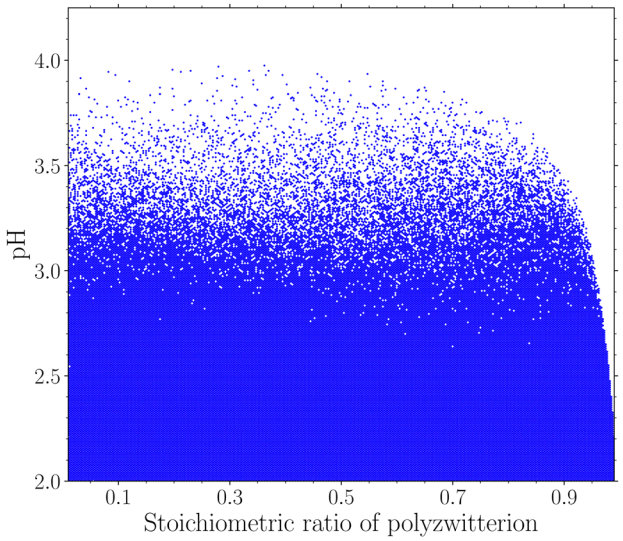

Fig. 6 Phase diagram for the baseline case. Each point indicates a set of stoichiometric ratio value and pH value in which complexation was found by the free energy minimization algorithm. The increasing sparsity of data points as pH increases indicates the growing instability of the pZC. Once the pH is sufficiently higher than the pK_a value, complexation can no longer be sustained.

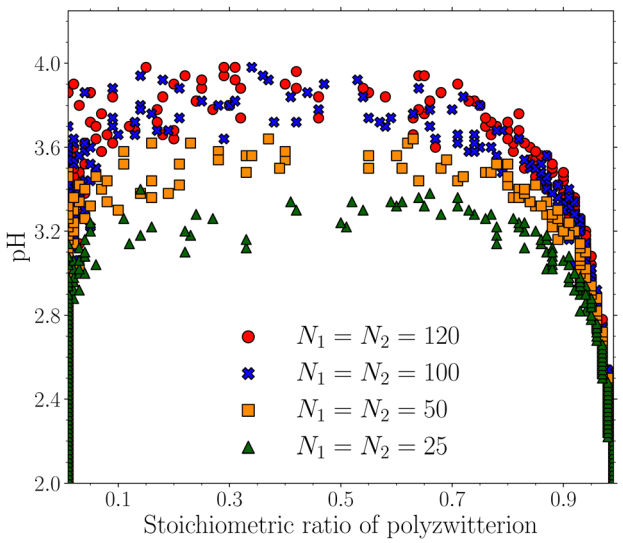

Fig. 7 Phase diagram for symmetric polymer chain lengths. Shorter chain lengths result in pZCs that have a smaller pH range for complexation. Increasing the chain lengths results in pZCs that are more robust to changes in pH but such behavior saturates once the chain lengths are both above 100 monomers.

absence of a point indicates the free energy minimization algorithm did not find complexation.

Looking at Fig. 6, one can envision an envelope that separates the homogeneous and heterogeneous regions. Above that envelope, where no or very few data points are present, the pZC is dissociated, the polyzwitterion and polydipole are in a single phase. Below that envelope, the pZC is still intact and exists within in one of the two phases. As the pH is increased, the pZC becomes increasingly unstable, represented by the progressive sparsity of data points. Our pZC model clearly displays the pH-dependent behavior that is seen experimentally.

The phase diagram has a leftward lean, which is likely due to the additional counterions from the polyzwitterion at higher stoichiometric ratios. Recall that the polydipole does not have counterions to release while the polyzwitterion has two counterions per zwitterionic monomer. Therefore, higher stoichiometric ratios result in stronger electrostatic screening effects than lower stoichiometric ratios at the same pH. As pH increases, and the polyzwitterion monomers begins to shed both counterions in order to adopt the dipolar state, the electrostatic interactions are further weakened by increased screening effects, causing the window of complexation (w.r.t. stoichiometric ratio) to contract. While the polyanion does not have an appreciable effect on the behavior of the pZC (this will be elaborated upon in what remains of this section), in certain conditions, such as this particular system, it is absolutely necessary to form robust pZCs. The steep downward curve on the right-hand side of the phase diagram indicates that the polyzwitterion cannot form robust complexes by themselves, in agreement with experimental observations. However, we do expect it to be possible that a sufficiently hydrophobic (Section 3.3) or strongly dipolar (Section 3.6) polyzwitterion could self-aggregate and form complexes on their own.

Fig. 6 indicates that it is possible for dipolar chains to self-aggregate. This finding in our calculations is due to our treatment of the electrolyte chains as fully condensed dipoles, and is consistent with experimental observations that show the aggregation of polyelectrolyte chains at low ionic strengths due to unscreened dipolar interactions.[69] We note that there is some stochasticity visible in the upper envelope of the phase diagram; this feature results from well-known limitations of the Nelder–Mead minimization algorithm, wherein calculations near certain boundaries require exponentially longer times and smaller steps between conditions to converge on a value.[70]

The relatively broad and flat feature of the phase envelope suggests that the amount of polyzwitterion is insignificant for any complexation to occur – potentially useful for cases in which the desired polyzwitterion is difficult or costly to synthesize. Of course, our model does not predict the extent of complexation. It could be true that there is less complexation occurring at lower stoichiometric ratios than at higher stoichiometric ratios or *vice versa*. However, our model strictly predicts whether complexation does or does not occur at a given stoichiometric ratio. The authors of the experimental work found that pH did affect the stoichiometric ratio in which peak complexation did occur. Simulation experiments could be a useful complement to these results to quantify the extent of complexation.

Interestingly, one can observe that there is some asymmetry in the behavior of this system, which can be explained by the fact that two independent processes with two different associated equilibria (namely, the acid–base equilibrium that controls the ionization of the backbone-proximal negatively charged group, and the salt condensation that controls the ionization of the distal positively charged group). At a given pH value, the contribution from the associative term between a

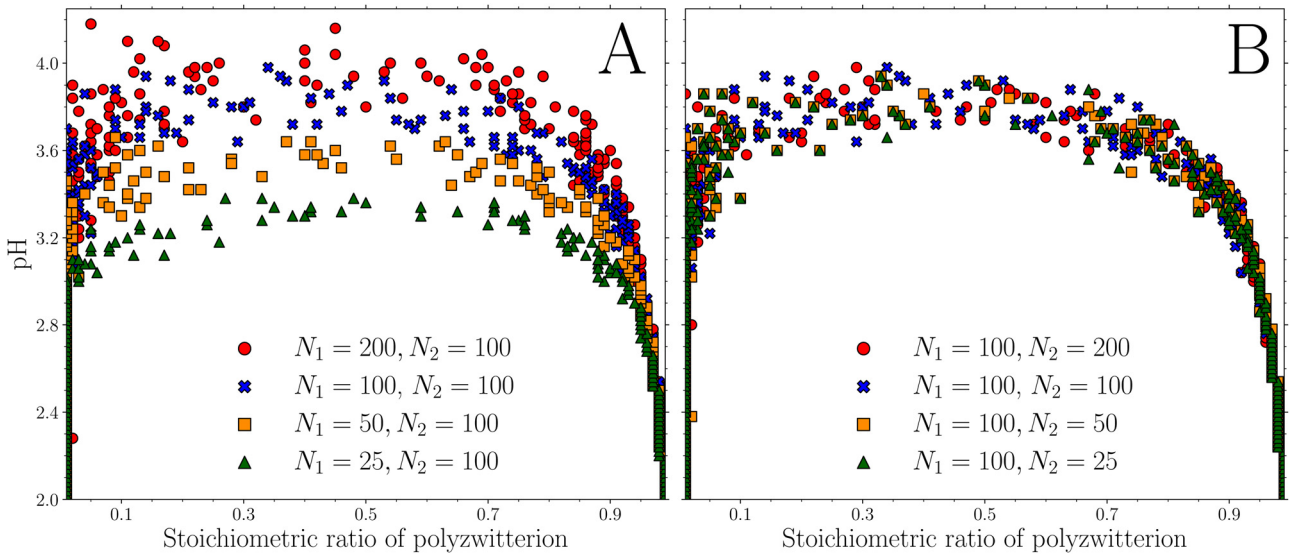

Fig. 8 Phase diagrams for asymmetrical polymer chain lengths. (A) Varying the chain length of the polyzwitterion while the polydipolechain length is fixed. (B) Varying the chain length of the polydipole while that of the polyzwitterion is held constant.

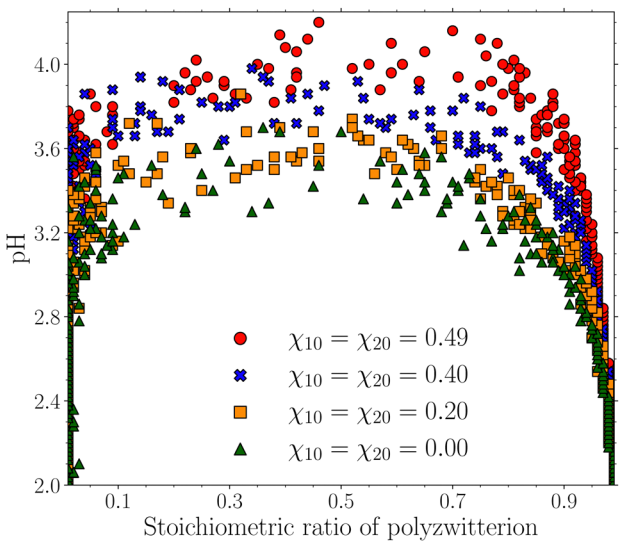

Fig. 9 Phase diagram for equally hydrophobic polymers. As the polymers are made increasingly hydrophobic, pZC formation increases along with it.

positive ion on the zwitterion and a dipole on the polydipole is attenuated by a negative charge on the zwitterion monomer on the opposite side of the positive charge; the proportion of each type of interaction is controlled simultaneously by the pK_a and the K_{salt}, and modulated as we vary the values of the pK_a and K_{salt} independently as we demonstrate below.[71]

For the following calculations in the remainder of this manuscript, we will use the parameters corresponding to the baseline case unless noted otherwise. For clarity, and to better ascertain the effects of the parameters, the outer envelope (constructed by taking the minimum and maximum stoichiometric ratios in which complexation is found at each pH value) of the phase diagram for each case will be plotted for the remainder of this manuscript. While this visualization method will invariably consider the sparse region where complexation is improbable, it will give the absolute boundary in which we no longer find complexation whatsoever.

3.2 Effect of chain length

3.2.1 Symmetric chain length modification. To evaluate how our pZC model responds to changes with respect to physical properties, we first modify the chain lengths symmetrically. We begin by considering different cases in which both polymer species are of equal lengths ($N_1 = N_2 = N$). Viewing Fig. 7, it is evident that the chain lengths only have an appreciable effect on the pZC phase behavior up to about $N = 100$. At $N = 200$, not shown here, there is no discernible difference in phase behavior compared to the case where $N = 120$. As the chain lengths increase, the pH range in which the pZC is stable broadens but quickly saturates. Polymer chain length only shows up explicitly in our free energy density expression in eqn (2) where each term in inversely proportionally scaled by its corresponding chain length. Within a physical picture, the polymers are confined to a smaller set of configurations which reduces their favorable translational entropic effects. As a result, the homogeneous system becomes less favorable, and the pZC is able to exist in a wider pH range. This finding is reminiscent of the roughly $1/\sqrt{N}$ dependence on the critical χ in the Flory–Huggins theory of mixing. This behavior can also be explained by decreasing contacts between individual polyzwitterion and polydipole chains as the chain lengths decrease, providing fewer points of contact for attractive electrostatic interactions.

3.2.2 Asymmetric chain length modification. Next, we will vary the chain length of one polymer while the chain length of the other is fixed to capture the individual effects arising from the polyzwitterion and polydipole. When we modify the

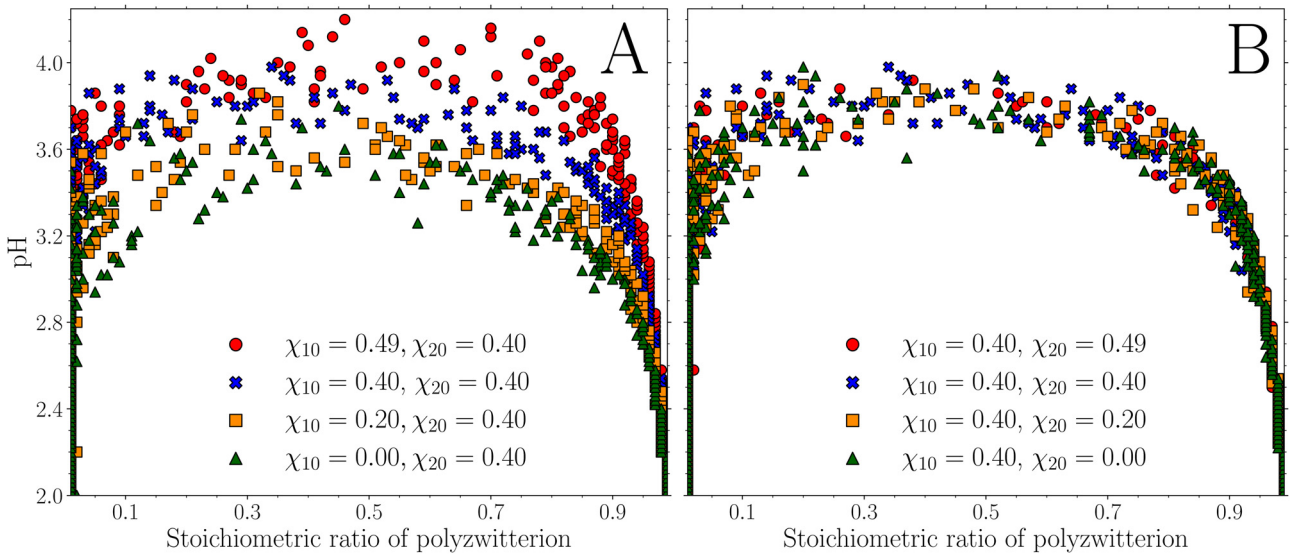

Fig. 10 Phase diagrams for unequally hydrophobic polymers. (A) The hydrophobicity of the polyzwitterion is varied while the hydrophobicity of the polydipole is constant. (B) The hydrophobicity of the polydipole is varied while that of the polyzwitterion is constant. Similar to the study of the chain lengths, the hydrophobicity of the polydipole does not significantly contribute to the overall phase behavior of the pZC.

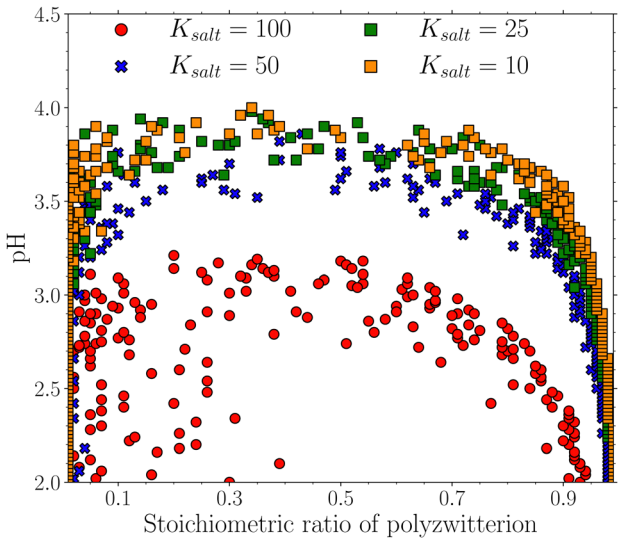

Fig. 11 Phase diagrams for various K_{salt} values of the permanently charged group on the zwitterion. (A) As K_{salt} increases, the permanently charged group is more likely to have a small negative salt ion condensed onto it thus suppressing the polyzwitterion's ability to be involved in charge–dipole electrostatic interactions that sustain pZC formation. (B) Complexation becomes less probable with decreasing stoichiometric ratio and increasing pH.

polyzwitterion chain length individually, we observe similar behavior to that of the congruous chain length modification. In fact, the effects are so similar to that it could lead one to wonder if the polydipole chain length has any influence on pZC phase behavior. Not surprisingly, our results show that it has no significant influence on the overall phase behavior of the pZC.

It is possible to glean from Fig. 8 that the number of dipoles along a polymer chain is not a phase-determining factor but rather the number of charged groups (whether they are quasi-cationic or -anionic) along the polymer chain. Let's say the pH is 2.5; from Fig. 3, the probabilities of each state are 0.60, 0.33, 0.01, and 0.06 for states A, B, C, and D, respectively. Concerning the polyzwitterion chain length, with N_1 = 25 roughly 8 monomers from each polyzwitterion chain are quasi-cationic, state C, and 15 are dipolar, state A. Now, with N_1 = 100, 33 monomers are quasi-cationic and 60 are dipolar. Conversely, when we vary the chain length of the polydipole, the number of dipoles on the polydipole chain scales linearly with N_2 while the number of charged monomers on the polyzwitterion remains the same. If the number of dipoles along the polymer chain was a factor, we would expect to see a difference in phase behavior between the cases where N_2 = 50 and N_2 = 100, where the difference between the number of dipoles along the polydipole chain (50 dipoles) is greater than the difference in the number of dipoles along the polyzwitterion chain when N_1 = 25 and N_2 = 100 (35 dipoles). Clearly, however, there is no such difference in phase behavior, leading us to believe that the number of charged monomers along the polyzwitterion plays a key role in pZC stability. This falls in line with our earlier thinking, that one of the primary factors leading to complexation is the number of contacts per chain between individual polyzwitterion and protonated polyanion chains; but we also reason that the type of contacts being made (charge–charge, charge–dipole, dipole–dipole) are important as well. As we will see later, these conclusions only hold for systems in which the polyzwitterion dipole moment is not strong enough for self-aggregation.

3.3 Effect of Flory–Huggins interaction parameter

3.3.1 Equal miscibility. The next chemical property of concern is the hydrophobicity of both the polyzwitterion and polydipole, realized in the Flory–Huggins interaction parameter χ. When $\chi_{ij} > 0$, species i and j prefer to interact with

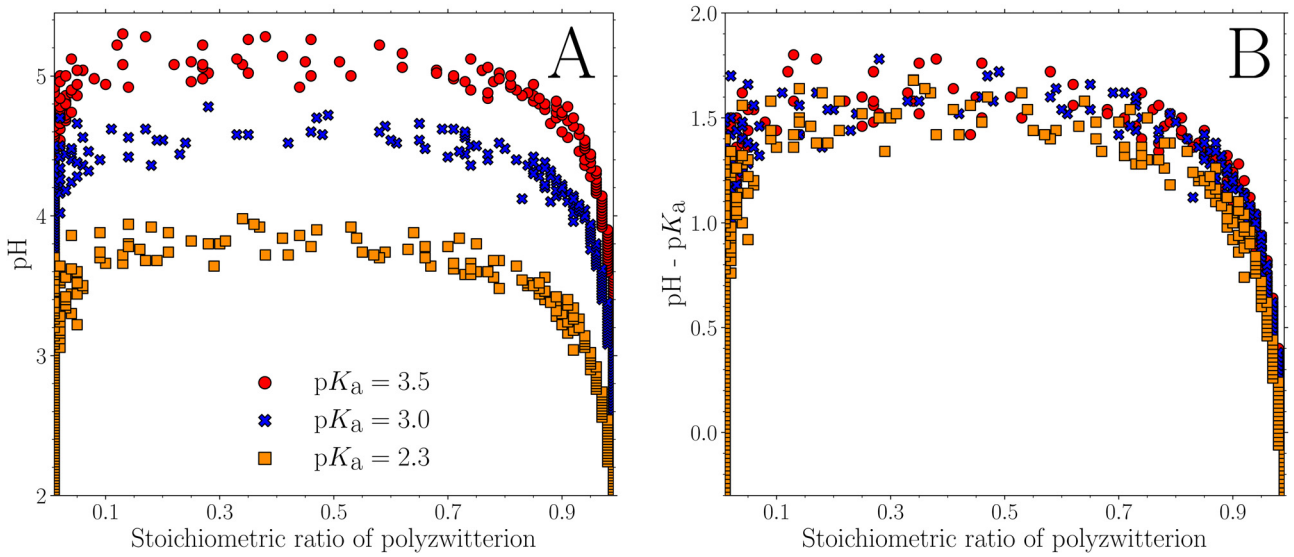

Fig. 12 Phase diagrams for various pK_a values of the pH-active charged group on the zwitterion. (A) As pK_a increases, the pZCs are able to sustain complexation into the higher pH range. (B) Visual inspection suggests that the difference between the curves correlate closely to the differences between the pK_a values. When the curves are aligned according to the difference between pH and their pK_a, no complexation is observed beyond 2 pH units above the pK_a of the negative moiety on the zwitterion for this particular system.

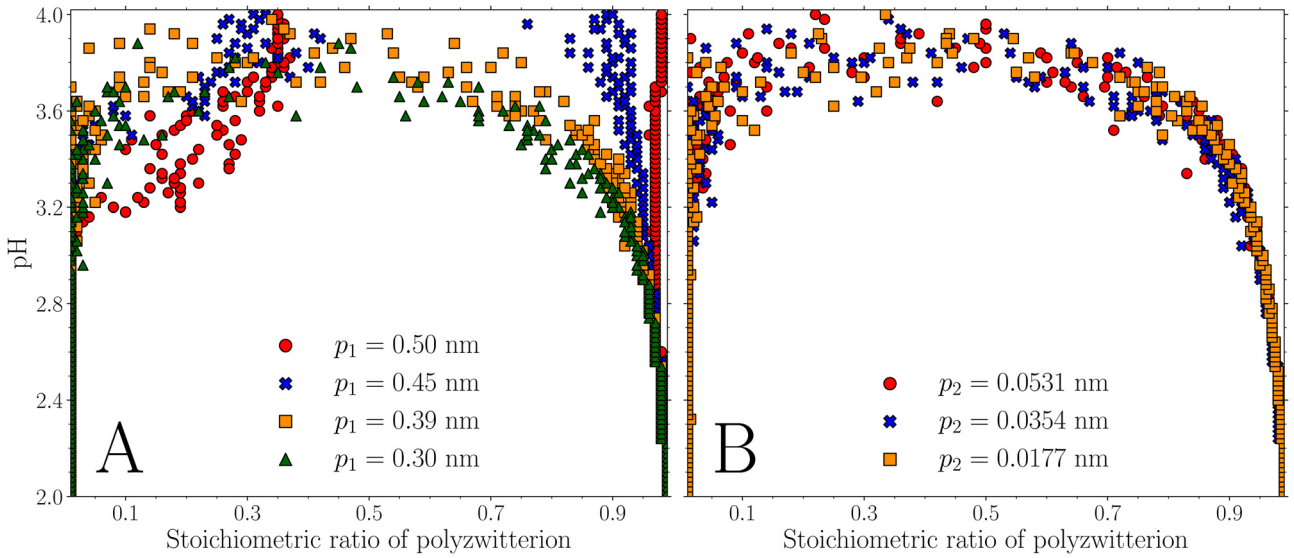

Fig. 13 Phase diagrams for various monomer dipole lengths. (A) The dipole length of the zwitterionic monomer is modified while that of the polydipole is fixed. Earlier discussion about long dipole lengths of the zwitterionic monomers allowing the formation of robust polyzwitterion–polyzwitterion complexes seems to confirmed. If the dipole length is long enough, when the primary mode of electrostatic interactions switches from charge–dipole to dipole–dipole, the latter will be sufficiently strong so as to sustain complexation even as the pH is 2 units about the pK_a value. (B) The dipole length of the polydipole is modified ±50% while the polyzwitterion dipole length is constant. The polydipole dipole length does not result in considerable difference in the window of complexation.

themselves through self-aggregation or complex with another polymer species (assuming the χ-parameter between those two species is not larger) rather than each other. Since we ignore chemical mismatch interactions involving ions and between the two polymer species, χ_{10} and χ_{20} define the hydrophobicity of the polyzwitterion and the polydipole, respectively. It is reasonable to believe that as we increase χ we will also increase the likelihood of pZC formation. Indeed, this is what we see in Fig. 9. As the hydrophobicity of each polymer is equally incremented, the pH range in which pZC formation occurs either expands or contracts as χ is increased or decreased, respectively. Surprisingly, however, we also see a slight swell in the right-hand side of the phase envelope, corresponding to the more polyzwitterion-rich mixtures, as χ is increased beyond our

baseline values of $\chi_{10} = \chi_{20} = 0.4$. This suggests that the hydrophobicity of the polyzwitterion has a stronger contribution to the pZC phase behavior than that of the polydipole, similar to what we saw with regards to chain lengths in the previous section. Increasing hydrophobicity also slightly widens the complexation window at higher stoichiometric ratios.

3.3.2 Mismatched Flory–Huggins interaction parameters. Next, we wish to elucidate if the phase behavior we see in Fig. 9 is due to the polyzwitterion, the polydipole, or some mixture of the two. Similar to the chain length study, we will fix the hydrophobicity of the polydipole while we vary that of the polyzwitterion, and *vice versa*. Again, what is observed, in Fig. 10, is that, with respects to hydrophobicity, the polyzwitterion largely determines the phase behavior of pZCs. Due to the increasing hydrophobicity of the polyzwitterion, the complexation window swells slightly in the higher stoichiometric ratio. With the swelling of the right-hand side of the complexation window with hydrophobicity in mind, one could imagine that if the polyzwitterion were to be made sufficiently hydrophobic, that the polyzwitterions could self-aggregate to form pZCs by themselves. However, in doing so, one loses the ability to use a relatively small amount of polyzwitterion for pZCs which could be prohibitive for costly and/or difficult to synthesize polyzwitterions. It is also unlikely that one would want such a poor solvent–solute pair.

In terms of practical guidance to those who want to synthesize pZCs with specific phase behavior, the hydrophobicity of the polyzwitterion chains appear to influence the phase behavior quite strongly. In other words, moderately hydrophobic polyzwitterions ($0 < \chi_{10} < 0.4$) would be better suited in scenarios where a broad, smooth window (w.r.t. stoichiometric ratio) of complexation is desirable. Conversely, in applications where a tightly-controlled pH response is required, hydrophilic or slightly hydrophobic polyzwitterions would be a better choice.

3.4 Effect of K_{salt} of the permanently charged group on the zwitterion

The next chemical property we investigated is the equilibrium constant of the salt condensation reaction that the permanently charged group of the zwitterion, the positive moiety, is subjected to. Based on the results from modifying the pK_a value, and keeping in mind that K_{salt} is the only other property that can alter the net charge of the polyzwitterion (Fig. 5C), we expect to see the pH range in which complexation occurs to be strongly determined by the value of K_{salt}. As K_{salt} increases, the products of eqn (2.5) (ESI,† Section S2) become more thermodynamically favorable. That is, more of the positive moieties on the polyzwitterion will be neutralized by small negative salt ions, decreasing the capability for the polyzwitterion to be involved in charge–dipole interactions. This behavior is evident in Fig. 4 through the amplification of state D and the suppression of state C.

Once again, the results bolster the hypothesis from the authors of ref. 40. In Fig. 11, complexation is considerably suppressed as the overall number of charged zwitterionic monomers decreases due to the increase in K_{salt}. Increasing K_{salt} from 25 to 100 results in a near twofold decrease in the number of charged zwitterionic monomers at the polyzwitterion's maximally charged state. Modifying K_{salt} to 10 and 50, using $K_{salt} = 25$ as the reference, the number of charged monomers increases by 24% and decreases by 16%, respectively, which accounts for the modest change in phase behavior relative to the $K_{salt} = 100$ case.

The broad smattering of data points in the lower stoichiometric ratios for the $K_{salt} = 100$ case is a result of the lack of robust pZC formation in that region. Similar to how polyzwitterion-polydipole complexation becomes less probable as pH is increased, complexation becomes less probable as we decrease the stoichiometric ratio for high values of K_{salt} (see Fig. 11B). This case looks very similar to the behavior seen when pH > 3.5 for the baseline case. It is possible that increasing K_{salt} effectively pushes the phase envelope downward with respect to pH. State D, the fully neutralized zwitterionic monomer state, dominates until roughly pH 2 to which then state A, the dipolar zwitterionic monomer state, becomes the dominant state. At no point is the majority of the electrostatic interactions that the polyzwitterion is involved in the pZC-sustaining charge–dipole interactions. However, the net charge of the polyzwitterion is sufficiently high such that some complexation is possible, especially in the polyzwitterion-rich mixtures, in contrast to the case when p$K_a = 1.5$ and no complexation occurs.

3.5 Effect of pK_a of the pH-active charged group on the zwitterion

We expect the negative logarithm of the acid dissociation constant, or pK_a, of the pH-active charged group – the negative moiety – on the zwitterion to have a dominating effect on the pH range in which complexation is observed. Based on the mechanism of charge–dipole *vs.* dipole–dipole interactions, one can imagine that the window in which complexation is favored is intrinsically determined by the pK_a value as it determines the net charge of the polyzwitterion. When it is charged, the polyzwitterion can participate in charge–dipole interactions, and when it is neutral, those interactions disappear, as with complexation.

Moreover, returning once more to our free energy expressions, we see that the specific value of α_- is set by the difference between the pH of the system and the pK_a value. Furthermore, it is worth considering what happens to the states of the zwitterionic monomers through the values of $\mathbb{R}_i$ (2nd column from the right in Fig. 4) and Q_1 (Fig. 5C) as the pK_a value shifts. Based on those two characteristics, we expect to see pZC formation cease as the polyzwitterion becomes net-neutral because its monomers adopt the dipolar state. The results in Fig. 12 agree with our expectation; the highest pH in which complexation occurred for each set of data closely corresponds to the pH in which nearly all zwitterionic monomers adopt the net-neutral, dipolar state.

We also considered the case where p$K_a = 1.5$ from pH 1 to pH 4 and found no complexation whatsoever. We believe this is primarily due to the low charging of the polyzwitterion over the

considered pH range (see Fig. 5C). The maximal charge of the polyzwitterion when pK_a = 2.3, 3.0, and 3.5 are +0.47, +0.73, and +0.84, respectively. However, when pK_a = 1.5, the maximal charge of the polyzwitterion is +0.06, roughly an order of magnitude lower than the above pK_a values. It is evident that the polyzwitterion can scarcely participate in the charge–dipole interactions that are necessary for complexation. However, complexation still occurs when $Q_1 \approx +0.02$ for the p$K_a \geq 2.3$ cases. The complete lack of pZC formation must also be partially due to the inversely proportional relationship between pH and volume fraction of salt ions – a decrease of one pH unit corresponds to an order of magnitude increase in the volume fraction of salt ions. When we set pK_a = 1.5, this is the only case in which we consider pH values below pH 2. Therefore, between the range of pH 1 to pH 2, this system is subjected to greater electrostatic screening than all the other cases. It should also be noted that the maximal charge of the polyzwitterion when pK_a = 1.5 occurs within that pH range. Thus, the lack of charge–dipole interactions combine with the increased electrostatic screening to suppress any complexation between pH 1 and pH 4 when pK_a = 1.5.

For this particular system, when the phase envelopes are shifted according to the difference between pH and pK_a, it is clear that complexation ceases when the pH of the system is more than 2 units above the pK_a. At such a relatively high pH, the polyzwitterion is essentially a chain of dipoles. It is also evident from the right-hand branch of the envelope that complexation begins to contract as the pH approaches the pK_a value sooner for zwitterions with lower pK_a. We also believe this is due to the stronger electrostatic screening at lower pH values. Zwitterions with lower pK_a values will stop complexation at lower pH values (*i.e.*, higher salt volume fractions). These results lend further credence to the arguments of the authors of the experimental work.

3.6 Effect of dipole lengths of the monomers

By varying the dipole lengths of the monomers of each polymer, we expect to see considerable shifts in the specific phase behavior of the pZCs because of the scaling of the dipole–dipole interactions with dipole length – that is, $f_{el,dd} \sim p_{i\in\{1,2\}}^4$. Keeping the mechanism of charge–dipole *vs.* dipole–dipole electrostatic interactions in mind, one should expect that if the dipole length of the zwitterionic monomer is increased, that complexation would be sustained for a broader pH range and that the window should widen. We see the former behavior but not the latter in Fig. 13A as the widening of the window does not occur. Rather, there is some necking behavior where the window of complexation contracts and shifts towards the more polyzwitterion-rich stoichiometric ratios. This behavior is similar to that seen with increasing hydrophobicity in the previous section. By strengthening the dipolar interactions, the polymer effectively becomes more hydrophobic as it will preferentially interact with itself, squeezing out progressively more water.[72]

As the dipole length of the zwitterionic monomer increases, complexation ceases at progressively lower pH values in the polyelectrolyte-rich polymeric mixtures, leading to the aforementioned necking behavior. At the same time, not only is the pH window of complexation pushed upwards, complexation can be induced at higher stoichiometric ratios. This is likely a result arising from the ratio between p_1 and ℓ. As the ratio between the dipole length of the zwitterionic monomer and the Kuhn segment length grows, interactions between adjacent chains will be correspondingly strengthened. That said, in the context of real systems, it is likely that choosing polyzwitterions with longer zwitterionic monomer dipole lengths will have a favorable effect on the formation of pZCs with a given polyelectrolyte, assuming the polymeric mixture is not too deficient of polyzwitterion.

A question arising from this physical picture is whether the increase in dipole length of the zwitterionic monomer is helpful or detrimental for complexation. A longer dipole length would likely increase the propensity for the exposed positive charge to interact closely with an electrolyte. Therefore, stronger dipole interactions would be expected for larger values of p_1, as evidenced by complexation being pushed into higher stoichiometric ratios, but it does not describe the behavior seen in polyelectrolyte-rich mixtures.

In response to these points, important implications about the present physical model need to be considered. If the picture is indicating that the penetration of the zwitterion's positive charge into the volume occupied by the protonated polyanion dictates the parameter space in which complexation occurs, one wonders if the starting assumption of freely rotating dipoles is accurate in describing every dipole in the system. In dilute conditions, a dipole in isolation at a high enough temperature should of course be expected to rotate freely. But when a dipole is in the neighborhood of a charge, perhaps that rotation is skewed such that the oppositely charged end of the dipole preferentially rotates towards that charge. If the charge and dipole are brought into even closer proximity, the association of the electron-rich end of a dipole and a positive charge becomes even more favorable. Furthermore, this picture does not consider the influence that the tethering of a dipole length close to a polymer backbone has on the phase behavior of the system. In the experimental work, the dipole length of the protonated electrolyte was both smaller, and existed in closer proximity to a polymer backbone than that of the polyzwitterion. Additionally, effects arising from the segment of the tether between the two charges on the zwitterion are not considered.

The hypothetical scenario in which the value of p_1 is so high that dipole–dipole interactions are strong enough to support complexation through this mechanism alone, regardless of whether or not charges are present in the system is borne out in Fig. 13A. An important implication is that at pH windows in which the charging of the polyelectrolyte becomes relevant (at pH values within $\sim$1 unit away from the polyelectrolyte pK_a value), further charge–dipole complexation may be possible, except this time the charge will arise from the polyelectrolyte proper, and the dipole will belong to the polyzwitterion. Of course, this scenario does not arise in either the experimental work or the current work. However, it is prudent to take

this possibility into consideration in future work that incorporates new chemistries into the synthesis of pZCs.

4 Conclusions and future work

In this work, we introduced a theoretical framework for polyzwitterion–polyelectrolyte complex coacervation that reasonably agrees with recent experimental work. By modeling the polyzwitterion as a combination of zwitterionic states, where the fraction of each polyzwitterion chain that belongs to each state is dependent upon chemical properties of the charged groups on the zwitterion and system conditions, we were able to capture the dynamic nature of the polyzwitterion with changing pH. We focused on the effects of experimentally relevant and synthetically modifiable parameters – such as degrees of polymerization, Flory–Huggins interaction parameters, pK_a of the pH-active charged group on the zwitterion, K_{salt} of the permanent charge group on the zwitterion, and dipole lengths – have on complexation over a range of pH values and stoichiometric mixing ratios of the polymers. Interestingly, the chemical and physical properties of the polyzwitterion are found to be the main driving force of the phase behavior of the pZCs. This finding should allow researchers to focus their attention on the specifics of the polyzwitterion, alleviating some of the leg work that would be necessary to select an appropriate polyelectrolyte complement (one just needs to select a polyelectrolyte with a sufficiently high pK_a value). Hopefully this work also spurs and guides further investigations into polyzwitterionic complexes.

With regards to molecular design for specific pZC phase behavior, one will find that they are able to brush in broad and fine strokes by carefully working within the correct parameter space. The chemical properties that directly dictate the ionization of the charged groups on each zwitterionic monomer – pK_a of the pH-active charged group and K_{salt} of the permanent charged group – have the most profound effect on pZC phase behavior by significantly altering the net charge of the polyzwitterion and the pH range over which it is charged. The dissociation of the pZC follows closely to the net-charge of the polyzwitterion, particularly when it approaches neutrality (*i.e.*, becomes a chain of dipoles). Obviously, the states of the zwitterionic monomers are quite important to the pH-sensitive behavior of pZCs, agreeing with experimental results. Given the augmentation of the complexation window with varying χ-parameters and dipole lengths (that is, the stoichiometric ratio dependence), we recommend using the degree of polymerization of the polyzwitterion to obtain finer control over pZC phase behavior. In summary, we recommend those interested in designing a pZC system to first select appropriate charged groups on the zwitterion to constrain the dissociation or association behavior to a small pH range. The polyzwitterion backbone should be moderately hydrophobic to achieve more consistent phase behavior across a range of stoichiometric values. For the same reason, ensure the dipole length of the polyzwitterion is not sufficiently close to the spacing between each zwitterionic monomer. Finally, one should then modify the molecular weight (*i.e.*, chain length) of the polyzwitterion to achieve the desire phase behavior.

Beyond molecular design, one can also consider similar systems with "blocky" regions in a single polymer chain, each block being zwitterionic, dipolar, or explicitly charged. Constructing free energy expressions for such systems is not particularly different from what is done in this work, in principle, so long as all the interactions are accounted for. However, going one step further, one can quickly realize that these blocky systems can be used to understand the aberrant phase separation of intrinsically disordered proteins in the human body. The condensation of α-synuclein is implicated in the pathophysiology of various illnesses, such as Parkinson's disease and Lewy Body dementia.[23–25] This protein can be modeled as a block copolymer, consisting of three regions: one charged, one dipolar, and one hydrophobic. Such a simplified model could allow researchers to investigate the behavior of these protein aggregates as a function of various useful chemical characteristics, which in turn could help illuminate some of the potential avenues by which aberrant phase separation in the biomedical context can be eliminated.

Further work investigating the suppression of polyzwitterion–polyelectrolyte complexation in polyelectrolyte-rich polymeric mixtures as the dipole length of the zwitterionic monomer is increased could elucidate the mechanism that dictates this phenomenon. Additionally, it is known that dipole orientation, whether the segmental dipole is pointed towards or away from the polymer backbone, influences the association of polyzwitterions,[73] but is not considered in this work. Further work could also highlight if continuing to raise the pH to values that are relevant to polyelectrolyte ionization will yield a re-entrant region. We expect that as pH is increased, the polyzwitterion will become a chain of dipoles while the polyelectrolyte becomes charged. Now, charge–dipole interactions will resume, and so should polyzwitterion–polyelectrolyte complex coacervation. We also hypothesize the complexation of polyzwitterion with polycation in basic conditions, a mirror image of the experimental system and model in this work. In the experimental system described in the introduction, the polyzwitterion associates with the polyelectrolyte at low pH. If the negative moiety on the zwitterion were permanent and the positive moiety a pH-active charge, it could, hypothetically, be possible to induce complexation at high pH using the mechanism described herein. Questions about the useful applicability of such a system aside, demonstrating the existence of such a system would further bolster the theory in this work and provide an additional chemical handle by which new phase behaviors can be elicited by polyzwitterion–polyelectrolyte systems.

Author contributions

S. C. H. and K. O. M. contributed equally to the work. M. M. supervised and provided funding for the project.

Data availability

The data presented in this study are openly available in the article.

Conflicts of interest

The authors declare no competing financial or non-financial interests.

Acknowledgements

We thank the National Science Foundation (DMR-2309539 and CHE-1904660) and AFOSR Grant FA9550-23-1-0584 for financial support. K. O. M. thanks the NSF for financial support from his National Traineeship grant (DGE-1545399). S. C. H. and K. O. M. also thank Siao-Fong Li for his useful discussions. S. C. H. thanks Jyoti Prakash Mahalik for training him to use the free energy minimization algorithm.

Notes and references

1 H. G. Bungenberg de Jong and H. R. Kruyt, *Proc. K. Ned. Akad. Wet.*, 1929, **32**, 849–856.
2 J. T. G. Overbeek and M. J. Voorn, *J. Cell. Comp. Physiol.*, 1957, **49**, 7–26.
3 Z. Ou and M. Muthukumar, *J. Chem. Phys.*, 2006, **124**, 1–11.
4 E. Spruijt, A. H. Westphal, J. W. Borst, M. A. Cohen Stuart and J. van der Gucht, *Macromolecules*, 2010, **43**, 6476–6484.
5 D. Priftis, X. Xia, K. O. Margossian, S. L. Perry, L. Leon, J. Qin, J. J. de Pablo and M. Tirrell, *Macromolecules*, 2014, **47**, 3076–3085.
6 C. E. Sing and S. L. Perry, *Soft Matter*, 2020, **16**, 2885–2914.
7 A. M. Rumyantsev, N. E. Jackson and J. J. De Pablo, *Annu. Rev. Condens. Matter Phys.*, 2021, **12**, 155–176.
8 P. Zhang and Z.-G. Wang, *Macromolecules*, 2022, **55**, 3910–3923.
9 C. E. Sing, *Adv. Colloid Interface Sci.*, 2017, **239**, 2–16.
10 M. Muthukumar, *Macromolecules*, 2017, **50**, 9528–9560.
11 X. Z. Shu and K. J. Zhu, *Int. J. Pharm.*, 2000, **201**, 51–58.
12 R. S. Riley, C. H. June, R. Langer and M. J. Mitchell, *Nat. Rev. Drug Discovery*, 2019, **18**, 175–196.
13 C.-H. Kuo, L. Leon, E. J. Chung, R.-T. Huang, T. J. Sontag, C. A. Reardon, G. S. Getz, M. Tirrell and Y. Fang, *J. Mater. Chem. B*, 2014, **2**, 8142–8153.
14 A. Murmiliuk, H. Iwase, J.-J. Kang, S. Mohanakumar, M.-S. Appavou, K. Wood, L. Almásy, A. Len, K. Schwärzer, J. Allgaier, M. Dulle, T. Gensch, B. Förster, K. Ito, H. Nakagawa, S. Wiegand, S. Förster and A. Radulescu, *J. Colloid Interface Sci.*, 2024, **665**, 801–813.
15 S. Lim, Y. S. Choi, D. G. Kang, Y. H. Song and H. J. Cha, *Biomaterials*, 2010, **31**, 3715–3722.
16 R. J. Stewart, C. S. Wang and H. Shao, *Adv. Colloid Interface Sci.*, 2011, **167**, 85–93.
17 R. J. Stewart, C. S. Wang, I. T. Song and J. P. Jones, *Adv. Colloid Interface Sci.*, 2017, **239**, 88–96.
18 B. Comiskey, J. D. Albert, H. Yoshizawa and J. Jacobson, *Nature*, 1998, **394**, 253–255.
19 Y. Chen, J. Au, P. Kazlas, A. Ritenour, H. Gates and M. McCreary, *Nature*, 2003, **423**, 136.
20 C. Schmitt and S. L. Turgeon, *Adv. Colloid Interface Sci.*, 2011, **167**, 63–70.
21 F. Shahidi, J. K. V. Arachchi and Y.-J. Jeon, *Trends Food Sci. Technol.*, 1999, **10**, 37–51.
22 T. Tanaka, C. Ishimoto and L. T. Chylack, *Science*, 1977, **197**, 1010–1012.
23 M. H. Polymeropoulos, C. Lavedan, E. Leroy, S. E. Ide, A. Dehejia, A. Dutra, B. Pike, H. Root, J. Rubenstein, R. Boyer, E. S. Stenroos, S. Chandrasekharappa, A. Athanassiadou, T. Papapetropoulos, W. G. Johnson, A. M. Lazzarini, R. C. Duvoisin, G. Di Iorio, L. I. Golbe and R. L. Nussbaum, *Science*, 1997, **276**, 2045–2047.
24 M. G. Spillantini, M. L. Schmidt, V. M.-Y. Lee, J. Q. Trojanowski, R. Jakes and M. Goedert, *Nature*, 1997, **388**, 839–840.
25 J. J. Zarranz, J. Alegre, J. C. Gómez-Esteban, E. Lezcano, R. Ros, I. Ampuero, L. Vidal, J. Hoenicka, O. Rodriguez, B. Atarés, V. Llorens, E. G. Tortosa, T. del Ser, D. G. Muñoz and J. G. de Yebenes, *Ann. Neurol.*, 2004, **55**, 164–173.
26 Y. R. Li, O. D. King, J. Shorter and A. D. Gitler, *J. Cell Biol.*, 2013, **201**, 361–372.
27 Y. Shin and C. P. Brangwynne, *Science*, 2017, **357**, eaaf4382.
28 S. Boeynaems, S. Alberti, N. L. Fawzi, T. Mittag, M. Polymenidou, F. Rousseau, J. Schymkowitz, J. Shorter, B. Wolozin, L. Van Den Bosch, P. Tompa and M. Fuxreiter, *Trends Cell Biol.*, 2018, **28**, 420–435.
29 S. Alberti, A. Gladfelter and T. Mittag, *Cell*, 2019, **176**, 419–434.
30 A. I. Oparin, *The Origin of Life*, Dover Publications, New York, New York, USA, 2nd edn, 1965.
31 W. M. Aumiller and C. D. Keating, *Nat. Chem.*, 2016, **8**, 129–137.
32 R. Booth, Y. Qiao, M. Li and S. Mann, *Angew. Chem., Int. Ed.*, 2019, **58**, 9120–9124.
33 K. K. Nakashima, M. H. I. van Haren, A. A. M. André, I. Robu and E. Spruijt, *Nat. Commun.*, 2021, **12**, 3819.
34 D. Priftis and M. Tirrell, *Soft Matter*, 2012, **8**, 9396–9405.
35 S. L. Perry, Y. Li, D. Priftis, L. Leon and M. Tirrell, *Polymers*, 2014, **6**, 1756–1772.
36 P. K. Jha, P. S. Desai, J. Li and R. G. Larson, *Polymers*, 2014, **6**, 1414–1436.
37 A. Salehi and R. G. Larson, *Macromolecules*, 2016, **49**, 9706–9719.
38 W. C. B. McTigue and S. L. Perry, *Soft Matter*, 2019, **15**, 3089–3103.
39 O. Adame-Arana, C. A. Weber, V. Zaburdaev, J. Prost and F. Jülicher, *Biophys. J.*, 2020, **119**, 1590–1605.
40 K. O. Margossian, M. U. Brown, T. Emrick and M. Muthukumar, *Nat. Commun.*, 2022, **13**, 2250.
41 J. K. Keum, P. Christakopoulos, Z. Liu, T. Li, J. Chen, A. Williams, D. K. Hensley, K. Hong, Y. Wang, R. Advincula and R. Kumar, *Eur. Polym. J.*, 2024, **215**, 113177.
42 S. Ganta, H. Devalapally, A. Shahiwala and M. Amiji, *J. Controlled Release*, 2008, **126**, 187–204.
43 E. Boedtkjer and S. F. Pedersen, *Annu. Rev. Physiol.*, 2020, **82**, 103–126.

44 E. Kokufuta, N. Shimizu and I. Nakamura, *Biotechnol. Bioeng.*, 1988, **32**, 289–294.
45 H.-C. Wang, Y. Zhang, C. M. Possanza, S. C. Zimmerman, J. Cheng, J. S. Moore, K. Harris and J. S. Katz, *ACS Appl. Mater. Interfaces*, 2015, **7**, 6369–6382.
46 Y. Zhang, Y. Han, Y. Lei, J. Ni, W. Zhou and Q. Xiao, *Batteries Supercaps*, 2024, e202400030.
47 H. Lambers, S. Piessens, A. Bloem, H. Pronk and P. Finkel, *Int. J. Cosmet. Sci.*, 2006, **28**, 359–370.
48 S. Jadoon, S. Karim, M. R. Akram, A. Kalsoom Khan, M. A. Zia, A. R. Siddiqi and G. Murtaza, *Int. J. Anal. Chem.*, 2015, **2015**, e164974.
49 M. Muthukumar, *J. Chem. Phys.*, 2004, **120**, 9343–9350.
50 M. Muthukumar, J. Hua and A. Kundagrami, *J. Chem. Phys.*, 2010, **132**, 084901.
51 A. R. Knoerdel, W. C. Blocher McTigue and C. E. Sing, *J. Phys. Chem. B*, 2021, **125**, 8965–8980.
52 S. Choi, A. R. Knoerdel, C. E. Sing and C. D. Keating, *J. Phys. Chem. B*, 2023, **127**, 5978–5991.
53 M. Muthukumar, *Physics of Charged Macromolecules: Synthetic and Biological Systems*, Cambridge University Press, Cambridge; New York, NY, 2023.
54 R. Staňo, J. J. van Lente, S. Lindhoud and P. Košovan, *Macromolecules*, 2024, **57**, 1383–1398.
55 S. Adhikari, M. A. Leaf and M. Muthukumar, *J. Chem. Phys.*, 2018, **149**, 163308.
56 G. S. Manning, *J. Chem. Phys.*, 1969, **51**, 924–933.
57 A. Kundagrami and M. Muthukumar, *J. Chem. Phys.*, 2008, **128**, 244901.
58 A. Kundagrami and M. Muthukumar, *Macromolecules*, 2010, **43**, 2574–2581.
59 J. D. Delgado and J. B. Schlenoff, *Macromolecules*, 2017, **50**, 4454–4464.
60 Z. J. Zhang, J. Madsen, N. J. Warren, M. Mears, G. J. Leggett, A. L. Lewis and M. Geoghegan, *Eur. Polym. J.*, 2017, **87**, 449–457.
61 S. Xiao, Y. Zhang, M. Shen, F. Chen, P. Fan, M. Zhong, B. Ren, J. Yang and J. Zheng, *Langmuir*, 2018, **34**, 97–105.
62 S. Xiao, B. Ren, L. Huang, M. Shen, Y. Zhang, M. Zhong, J. Yang and J. Zheng, *Curr. Opin. Chem. Eng.*, 2018, **19**, 86–93.
63 K. Qu, Z. Yuan, Y. Wang, Z. Song, X. Gong, Y. Zhao, Q. Mu, Q. Zhan, W. Xu and L. Wang, *ChemPhysMater*, 2022, **1**, 294–309.
64 S. Javan Nikkhah and M. Vandichel, *ACS Eng. Au*, 2022, **2**, 274–294.
65 J. Landsgesell, L. Nová, O. Rud, F. Uhlík, D. Sean, P. Hebbeker, C. Holm and P. Košovan, *Soft Matter*, 2019, **15**, 1155–1185.
66 C. G. Malmberg and A. A. Maryott, *J. Res. Natl. Bur. Stand.*, 1956, **56**, 1–8.
67 R. Lewis Sr., *Hawley's Condensed Chemical Dictionary*, John Wiley & Sons, Ltd, 16th edn, 2016, ch. 19, pp. 1197–1300.
68 J. A. Nelder and R. Mead, *Comput. J.*, 1965, **7**, 308–313.
69 M. Muthukumar, *Proc. Natl. Acad. Sci. U. S. A.*, 2016, **113**, 12627–12632.
70 J. C. Lagarias, J. A. Reeds, M. H. Wright and P. E. Wright, *SIAM J. Optim.*, 1998, **9**, 112–147.
71 R. Lunkad, A. Murmiliuk, P. Hebbeker, M. Boublík, Z. Tošner, M. Štěpánek and P. Košovan, *Mol. Syst. Des. Eng.*, 2021, **6**, 122–131.
72 R. Kumar, B. G. Sumpter and M. Muthukumar, *Macromolecules*, 2014, **47**, 6491–6502.
73 S. Morozova, G. Hu, T. Emrick and M. Muthukumar, *ACS Macro Lett.*, 2016, **5**, 118–122.